

Core-Controlled Formation of Micellar Cubic Assemblies of Supramolecular Dendrimers: From Their Mechanism to Formation of Gold Nanostructures

Seong A Kim, Dae-Hwan Jung, Yun-Ho Kim, Min Ah Kang, and Hee-Tae Jung*

Department of Chemical & Biomolecular Engineering (BK-21), Korea Advanced Institute of Science and Technology, 373-1 Guseong-dong, Yuseong-gu, Daejeon 305-701, Korea

Received May 13, 2006; Revised Manuscript Received July 11, 2006

ABSTRACT: We prepared gold nanostructures from a taper-shaped supramolecular material (1-COOH) containing a carboxylic acid (–COOH) core, rigid biphenylene group, and three perfluorinated (–CF₃) tails. The carboxylic core of the supramolecule serves as the site for reaction with the metal ions. We show that the self-assembling behavior of the material is strongly affected by substituting the carboxylic core of the supramolecule with a Na⁺ ion, followed by ion transfer of Au^{III} and subsequent reduction of Au^{III} with UV irradiation. Synchrotron X-ray diffraction (XRD) results show that the structure of 1-COOH solution (THF) and [1-COO[–]–Na⁺] complex is disordered. However, the [1-COO[–]–Au^{III}Cl₃][–] complex before UV irradiation exhibits liquid crystalline order with micellar cubic assemblies. This order and spacing are preserved during reduction of the metal salt with UV irradiation, although the intensities of the peaks increase. UV–visible spectra and transmission electron microscopy (TEM) images show the generation of the gold arrays in the presence of the supramolecular building block. Moreover, the size and shape of gold nanocrystals are controllable depending on UV irradiation time. These types of perfluorinated supramolecular templates have enhanced mesophase stability on account of the existence of strong intermolecular interactions, although many of these molecules are not traditional amphiphiles.

Introduction

Self-assembling materials such as surfactants, colloids, block copolymers, and supramolecules have been proposed as potential materials for the template-directed creation of inorganic nanostructure due to their ability to self-aggregate into nanometer-scale building blocks.^{1–7} In such systems, the controlled fabrication of nanoscopic fillers at defined positions within the building blocks is essential to realizing periodically patterned templates. For examples, block copolymers with features of the order of 5–100 nm, depending on the molecular weight of the copolymer and the strength of the segmental interaction between the blocks, have been used as templates to fabricate various metals and semiconducting materials.^{8–10} The resultant inorganic encapsulated block copolymers have potential applications such as optoelectronics, chemical sensors, electroluminescent and photoluminescent diodes, catalysts, selective membranes, and high-performance engineering materials. Similar approaches have been reported in other self-assembling building blocks. As yet, however, very few attempts have been made to generate inorganic nanostructure using supramolecular templates, largely due to the difficulty of placing and immobilizing the nanoscopic fillers at predefined positions afforded by the periodic arrays of supramolecular liquid crystals, although the ability to reduce feature size is superior to that of block copolymers. Unlike the case of other self-assembling materials, furthermore, a more systematic approach is required to obtain such inorganic nanostructures because the structure and stability of these taper-shaped supramolecules are very sensitive to the nature of their core groups.^{7,11,12}

Here we present perfluorinated supramolecules containing a carboxylic acid (–COOH) core, rigid biphenylene group, and three perfluorinated (–CF₃) tails as the template material for

the fabrication of 1D and 2D gold nanocrystals of adjustable size, order, and shape. We found that the structure was changed with different core molecules through an ion transfer reaction and photoreduction of a gold salt (Au^{III}) in the solution phase of the taper-shaped supramolecule. Micellar cubic assemblies start to form by converting a carboxyl core into the gold ions before UV irradiation, and the structure is preserved during reduction of the metal salt with UV irradiation.

Experimental Section

Materials. The supramolecule (3,5-bis[3',5'-bis(*n*-5,5,6,6,7,7,8,8,9,9,10,10,11,11,12,12-heptafluorododecan-1-yloxy) benzyloxy]benzoic acid), which we denote as 1-COOH, was synthesized by etherification of the intermediate alcohols with the corresponding biphenylmethyl chloride, which was prepared via the reduction (LiAlH₄) and chlorination (SOCl₂) of an as-prepared perfluorinated biphenyl ester precursor. 1H,1H,2H,2H,3H,3H,4H,4H-perfluorododecyl bromide was prepared by (Ph₃P)₄Pd(0)-catalyzed radical addition of *n*-perfluorooctyl iodide to vinyl acetic acid, reduction of the iodo and carboxylic group carried out in a single step with LiAlH₄, and bromination of carbon tetrabromide catalyzed by triphenylphosphine after purification by sublimation. Alkylation of methyl 3,5-dihydroxybenzoate with 1H,1H,2H,2H,3H,3H,4H,4H-perfluorododecyl bromide in DMF at 65 °C with K₂CO₃ as a base yielded after 8 h, which was then purified by flash column chromatography (SiO₂, 2:1 hexane/ethyl acetate). The synthesized methyl 3,5-bis(*n*-5,5,6,6,7,7,8,8,9,9,10,10,11,11,12,12-heptafluorododecan-1-yloxy) benzoate was reduced by LiAlH₄ and chlorinated by SOCl₂ in CH₂Cl₂ and THF for 20 min. After the purification of methyl 3,5-bis(*n*-5,5,6,6,7,7,8,8,9,9,10,10,11,11,12,12-perfluorododecyl bromide by flash column chromatography (SiO₂, 2:1 hexane/ethyl acetate), alkylation of the methyl 3,5-dihydroxybenzoate of methyl 3,5-bis(*n*-5,5,6,6,7,7,8,8,9,9,10,10,11,11,12,12-heptafluorododecan-1-yloxy)benzyl chloride was performed following the procedure outlined above. Hydrolysis of the methyl ester group of methyl 3,5-bis[*p*-(*n*-5,5,6,6,7,7,8,8,9,9,10,10,11,11,12,12-heptafluorododecan-1-yloxy)benzyloxy] benzoate with KOH/EtOH at reflux produced 3,5-

* Corresponding author. E-mail: heetae@kaist.ac.kr. Web: <http://oem.kaist.ac.kr>.

bis[*p*-(*n*-5,5,6,6,7,7,8,8,9,9,10,10,11,11,12,12,12-heptadecafluorododecan-1-yloxy)benzyloxy] benzoic acid. ^1H NMR (300 MHz [D_8] THF, 25 °C, TMS, Supporting Information): 1.73 (m, 16H, $\text{CF}_2\text{-CH}_2(\text{CH}_2)_2$), 2.17 (m, 8H, CF_2CH_2), 3.90 (t, 8H, $\text{CH}_2\text{CH}_2\text{CH}_2\text{OAr}$, $J = 5.83$ Hz), 4.92 (s, 4H, ArCH_2OAr , 3,5-positions), 6.32 (s, 2H, ArH meta to CH_2OAr , 4-position), 6.51 (s, 4H, ArH ortho to $\text{CH}_2\text{-OAr}$, 2,6-positions), 6.72 (s, 1H, ArH meta to COOCH_3 , 4-position), 7.16 (s, 2H, ArH ortho to COOCH_3 , 2,6-positions). ^1H NMR (300 MHz, [D_8] THF, 25 °C, TMS): $\delta = 1.73$ (m, 16H, $\text{CF}_2\text{CH}_2(\text{CH}_2)_2$), 2.17 (m, 8H, CF_2CH_2), 3.90 (t, ${}_3J(\text{H,H}) = 5.83$ Hz, 8H, $\text{CH}_2\text{-CH}_2\text{CH}_2\text{OAr}$), 4.92 (s, 4H, ArCH_2OAr , 3,5-positions), 6.32 (s, 2H, ArH meta to CH_2OAr , 4-position), 6.51 (s, 4H, ArH ortho to $\text{CH}_2\text{-OAr}$, 2,6-positions), 6.72 (s, 1H, ArH meta to COOCH_3 , 4-position), 7.16 (s, 2H, ArH ortho to COOCH_3 , 2,6-positions).

Preparation of Gold Nanostructure. The ordered gold nanostructures were prepared as follows: 1-COOH (0.01 mmol, 22.9 mg; 0.02 mmol, 45.9 mg) was dissolved in THF (6 mL) with two different molar ratios ($\text{HAuCl}_4/1\text{-COOH} = 1:1$ or $1:2$). To convert the carboxylic acid core of 1-COOH into a sodium salt, an aqueous solution of NaOH (200 μL , 0.01 mmol, 0.39 mg; 0.02 mmol, 0.78 mg) was slowly added dropwise with vigorous stirring into the 1-COOH solution (THF). The solution turned turbid at the start of addition, and then cleared slowly after sufficient stirring. To this solution, HAuCl_4 aqueous solution (2 mL; 0.01 mmol, 3.93 mg) was slowly added, and the resulting mixture was agitated for several hours to complete the complexation. HAuCl_4 aqueous solution was also slowly added to the resulting yellow solution to synthesize Au^{III} salts of the 1-COOH via ion exchange of Na^+ and Au^{III} with vigorous stirring. After the addition was complete, the solutions were transferred to quartz cells and directly irradiated with a 200 W low-pressure mercury UV lamp ($\lambda = 254$ nm) for 24, 36, or 48 h. Upon UV irradiation, the yellow color of the solution gradually disappeared such that, by 12 h, the solution was colorless. On further irradiation, the color of the solution became pinkish, and gradually changed from bright-pink into violet upon completion of the reduction.

Characterization. FT-IR spectra were obtained using a Bruker Tensor series 27 FT-IR spectrometer to confirm the reconstitution of the core. UV-vis spectra of the solutions were measured on a Varian Cary series 100 spectrometer. XRD measurements of the bulk and solution phases were performed using a synchrotron beam source at the 4C1 (Small-Angle X-ray Scattering Beamline I) and 4C2 (Small-Angle X-ray Scattering Beamline II) X-ray beam lines with $\lambda = 0.154$ nm at the Pohang Light Source (PLS), which has a 2.5 GeV LINAC accelerator. For these measurements, a small amount of sample in the liquid phase was sealed with imide films. High-resolution TEM images and electron diffraction were examined using a TEM (Philips F-20 FE-TEM) at a low-dose condition.¹³ TEM specimens were prepared as dispersed solutions on a carbon-supported TEM grid.

Results and Discussion

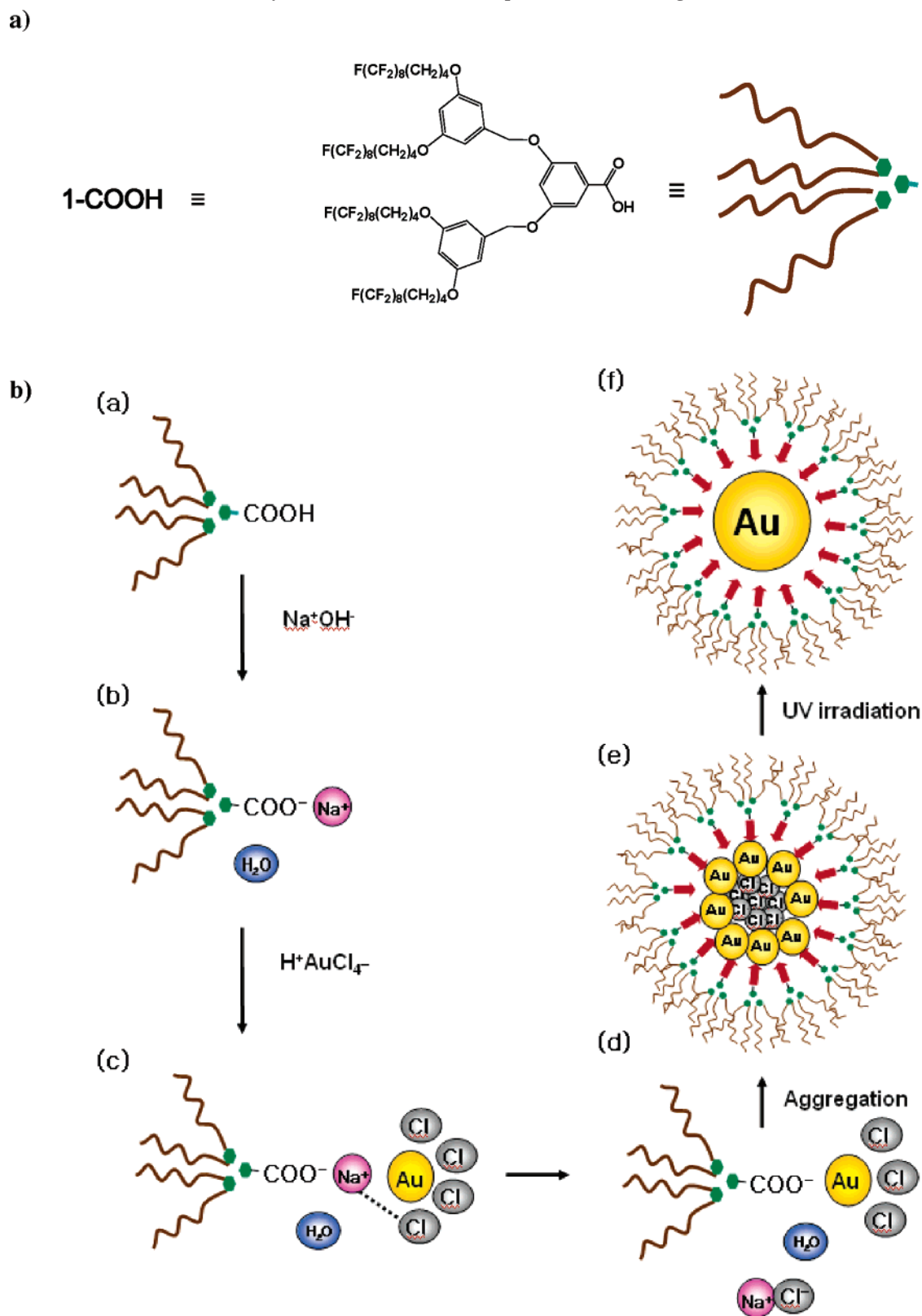
To realize this strategy, we synthesized a taper-shaped supramolecule containing a carboxylic core ($-\text{COOH}$), aromatic rings, and four perfluorinated ($-\text{CF}_3$) tails. This material forms a hexagonal columnar structure at the bulk phase (see schematic illustration of the overall synthetic procedures and characterizations in Supporting Information), while different mesophases are generated at the solution phase. Scheme 1 shows the fabrication scheme for creating the gold nanoarrays in the presence of the supramolecular self-assembly. To reconstitute the core segments of the material, we initially attempted to convert 1-COOH into $[1\text{-COO}^--\text{Na}^+]$ by treatment with NaOH (aq) solution. Briefly, an aqueous solution of NaOH was slowly added dropwise at room temperature to the 1-COOH dissolved in THF. An aqueous solution of HAuCl_4 was then slowly added to this solution, and the resulting mixture was agitated for several hours to complete the complexation of $[1\text{-COO}^--\text{Au}^{\text{III}}\text{Cl}_3]^-$. The resulting yellow solution was irradiated with UV light to

reduce the gold ions in the 1-COOH matrix. Upon UV irradiation, the yellow color of the solution gradually disappeared such that, by 12 h, the solution was colorless. On further irradiation, the color of the solution became pinkish and gradually changed from bright-pink into violet upon completion of the reduction. The conversion of 1-COOH into $[1\text{-COO}^--\text{Au}^{\text{III}}\text{Cl}_3]^-$ was confirmed by FT-IR spectroscopy (Figure 1). The peak associated with the C=O band of the carboxylic core was observed in the region of $1715\text{--}1680\text{ cm}^{-1}$. Loss of the absorption peak at 1690 cm^{-1} after adding NaOH (aq) indicates that the carboxylic group of the perfluorinated supramolecule was successfully converted into a salt of $[1\text{-COO}^--\text{Na}^+]$ (Figure 1b). After sufficient stirring, Au^{III} ions (aq) formed a salt with the material by ion exchange reaction (Figure 1c).¹⁴

To elucidate the structural changes that occurred at each stage, we investigated X-ray scattering experiments using synchrotron XRD (Figure 2): 1-COOH in THF, $[1\text{-COO}^--\text{Na}^+]$ complex, $[1\text{-COO}^--\text{Au}^{\text{III}}\text{Cl}_3]^-$ complex before UV irradiation, and 1-COOH-Au after UV irradiation. The XRD data for the 1-COOH solution (THF) and $[1\text{-COO}^--\text{Na}^+]$ complex show no specific reflections, indicating that the structure at this resolution is fully disordered. Clear reflection peaks appear from the $[1\text{-COO}^--\text{Au}^{\text{III}}\text{Cl}_3]^-$ complex before UV irradiation, indicating evidence of liquid crystalline order. In other words, the individual taper-shaped molecules start to self-assemble into an ordered state upon the conversion of 1-COOH into $[1\text{-COO}^--\text{Au}^{\text{III}}\text{Cl}_3]^-$. As HAuCl_4 aqueous solution was dropped into the 1-COOH solution and the amount of water was increased, the formation of micelles was started with hydrophilic interiors and hydrophobic exteriors. This order and spacing are preserved during reduction of the metal salt with UV irradiation, although the intensities of the peaks increase. The X-ray crystallographic analysis of 1-COOH-Au composites show that the ordered Au nanocomposites self-assemble into micellar cubic structure with face-centered cubic (fcc) packing ($a = 7.1$ nm; Table 1).^{15,16} As a result, the supramolecular core containing the gold salt acts as a template structure for the formation of ordered Au nanocrystals.

The UV-vis spectrum of the 1-COOH solution (THF) showed characteristic absorption maxima at 298 and 302 nm in the absence of HAuCl_4 , and no absorption bands in the range of 400–700 nm (Figure 3a). The AuCl_4^- ions in water exhibit an absorption peak at 319 nm that can be attributed to the metal-to-ligand charge transfer (MLCT) band of AuCl_4^- complexes.^{10,14,16} Addition of an aqueous HAuCl_4 solution to the $[1\text{-COO}^--\text{Na}^+]$ solution (THF) causes the 320 nm absorption band of AuCl_4^- complex and the 298 and 302 nm absorption band of the supramolecule to vanish due to AuCl_4^- complexes. A new absorption band with a shoulder, corresponding to the ion pair $[1\text{-COO}^--\text{Au}^{\text{III}}\text{Cl}_3]^-$, was observed at 337 nm.¹⁷ Upon UV irradiation, a peak at ~ 550 nm appeared, which can be assigned to the surface plasmon resonance on peak of nanosize Au^0 . This plasmon peak is slightly red-shifted with respect to the range typically observed for gold nanoparticles (510–525 nm), possibly due to the length and volume fraction of the stabilizing shell. Specifically, as the chain length and volume fraction of the stabilizing shell increases, the absorption band for aqueous colloidal gold nanoparticles of Au^0 will gradually shift to lower energy due to the contribution of the dielectric of the organic shell. In the case of 1-COOH-Au, the dense shell of binding ligands provides a dielectric coating on the particle surface, which effectively increases the dielectric constant of the medium, causing a red-shift in the absorption band.¹⁴ The intensity of the surface plasmon absorption peak of the gold

Scheme 1. Schematic Illustration of the Synthesis of Perfluorinated Supramolecular Building Block-stabilized Gold Nanocomposites



(a) Molecular architecture of the perfluorinated dendrimers synthesized in this study; (b) Schematic representation of the formation of gold nanoparticles within the supramolecular template.

nanoparticles was found to increase with increasing UV irradiation time (Figure 3b).

Figure 4 shows a representative high-resolution TEM image of individual gold nanocrystals deposited on a carbon-supported copper substrate. The samples fabricated with our method have a cubic arrangement, with the (111) planes oriented parallel to

the substrate (Figure 1a). The particles are spherical in shape and highly monodisperse, with a mean diameter and center-to-center distance of $\sim 4.0 \pm 0.5$ nm and 7.0 ± 0.5 nm, respectively, as determined by averaging measurements of approximately 300 gold particles taken from many different TEM images (molar ratio $\text{HAuCl}_4/1\text{-COOH} = 1:2$, UV irradiation

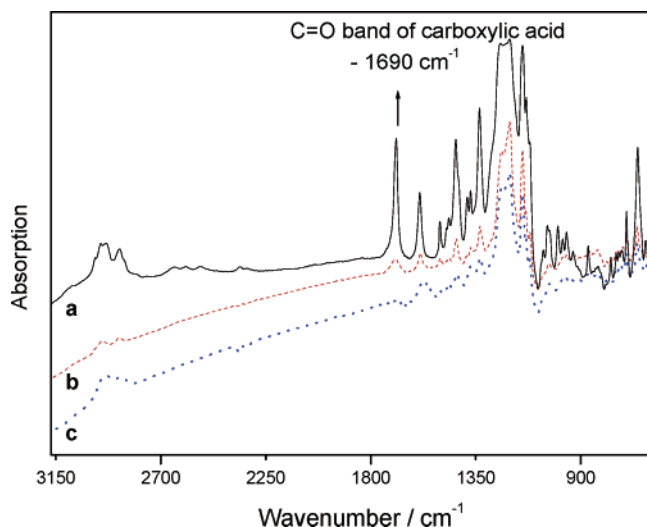


Figure 1. FT-IR spectra of (a) 1-COOH dissolved in THF (black), (b) after addition of NaOH aqueous solution to the 1-COOH in THF (red), and (c) after addition of HAuCl₄ aqueous solution to [1-COO⁻ - Na⁺] composite (blue).

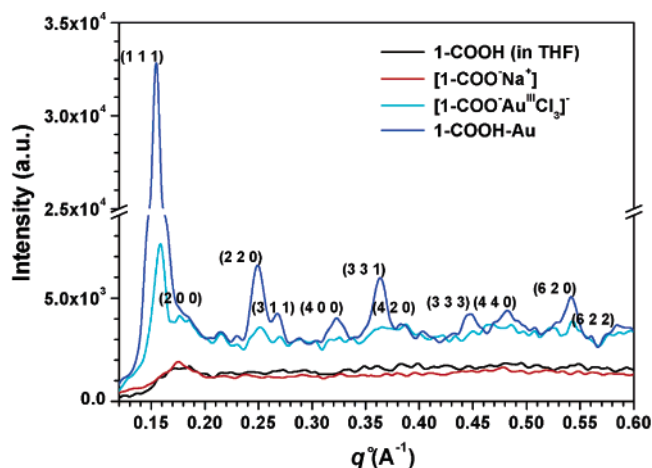


Figure 2. XRD pattern of the perfluorinated supramolecular building block-stabilized gold nanocomposites at each stage: 1-COOH solution (THF) (black), [1-COO⁻ - Na⁺] complex (red), [1-COO⁻ - Au^{III}Cl₃]⁻ complex before UV irradiation (green), and after UV irradiation (blue).

Table 1. Indexing Result ($a = 7.1$ nm)

(hkl)	$q_{\text{obs}}/\text{\AA}^{-1}$	$q_{\text{cal}}/\text{\AA}^{-1}$
(111)	0.1531	0.1531
(200)	0.1768	0.1768
(220)	0.2476	0.2500
(311)	0.2672	0.2931
(400)	0.3258	0.3535
(331)	0.3617	0.3852
(420)	0.3953	0.3953
(333)	0.4464	0.4593
(440)	0.4790	0.5000
(620)	0.5409	0.5590
(622)	0.5898	0.5863

tion for 48 h). This result is in excellent quantitative agreement with the XRD results. The average particle size increases with increasing UV irradiation time, from 3.0 ± 0.5 nm after 24 h of UV irradiation, to 4.0 ± 0.5 after 48 h, and to 9.0 ± 0.5 nm after 72 h. In particular, it is interesting that the observed distance between nearest-neighbor nanoparticles (2.5–3 nm) is considerably less than twice the calculated length of a fully extended 1-COOH (~ 2.1 nm),¹⁷ indicating that the rigid tail groups of the neighboring molecules likely interpenetrate each other to form the regular structures (Figure 4c). In addition, we

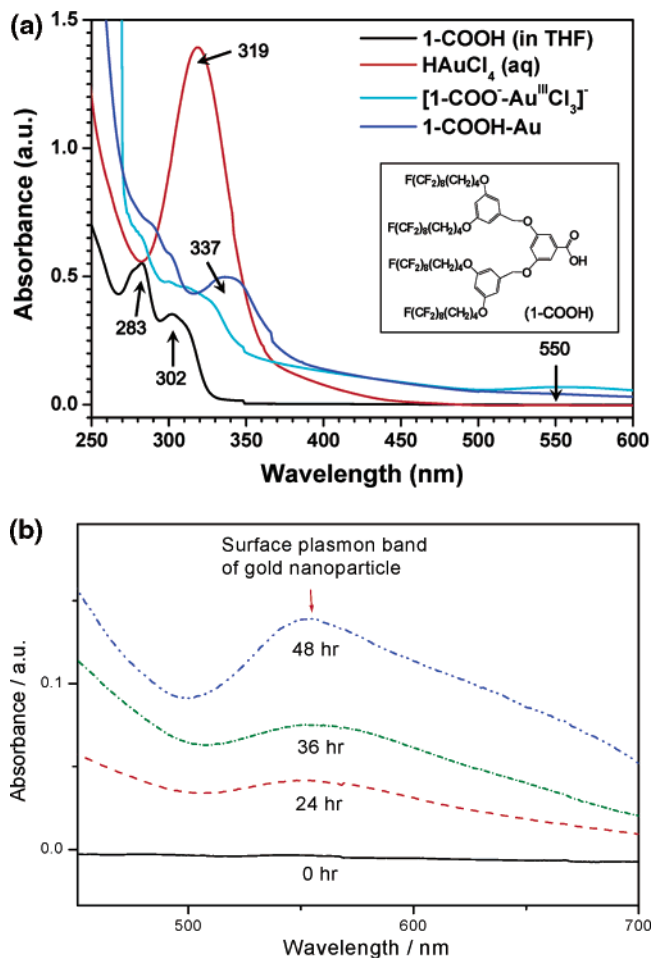


Figure 3. (a) UV-visible absorption spectra recorded at each stage during the synthesis of the perfluorinated supramolecular building block-stabilized gold nanocomposites: 1-COOH solution (black), HAuCl₄ (aq) (red), after addition of HAuCl₄ (aq) to [1-COO⁻ - Na⁺] (cyan), and after UV irradiation of the mixture (blue). (b) UV-visible absorption spectra at different UV irradiation times: THF (black), 24 h (red), 36 h (green), 48 h (blue).

found that the particle aggregation is strongly influenced by the molar ratio HAuCl₄/1-COOH of the complex. When the molar ratio was lower than 2, the gold nanoparticles aggregated to form lumps with dimensions on the order of hundreds of nanometers. This indicates that, at low molar ratios, the passivation groups of 1-COOH are insufficient for the gold nanoparticles to be stable and thus cannot keep the particle size in the nanometer range.

It is important to note that the gold nanoparticles coexist with nanofibers and nanoplates after 72 h, as clearly shown in Figure 4b, although the growth mechanism is not fully understood. The identification of the gold nanocrystals that form at molar ratios above 2 is made clear by examination at higher magnification (Figure 4, inset). The measured regular d -spacing of the observed planes of the lattice is 2.36 ± 0.02 Å, which corresponds to the spacing between the {111} planes of crystalline Au (2.355 Å). Because the 1-COOH template can be removed by many organic solvents, gold nanocrystals can be easily fabricated using these types of supramolecular dendrimers.

Unlike the case of conventional amphiphilic molecules containing strong hydrophilic headgroups and hydrophobic tails, these perfluorinated supramolecules are highly microphase separated around the centers of their carboxylic core groups and spontaneously self-organize into a hexagonal cylindrical structure in the bulk state.^{18,19} However, these supramolecules behave

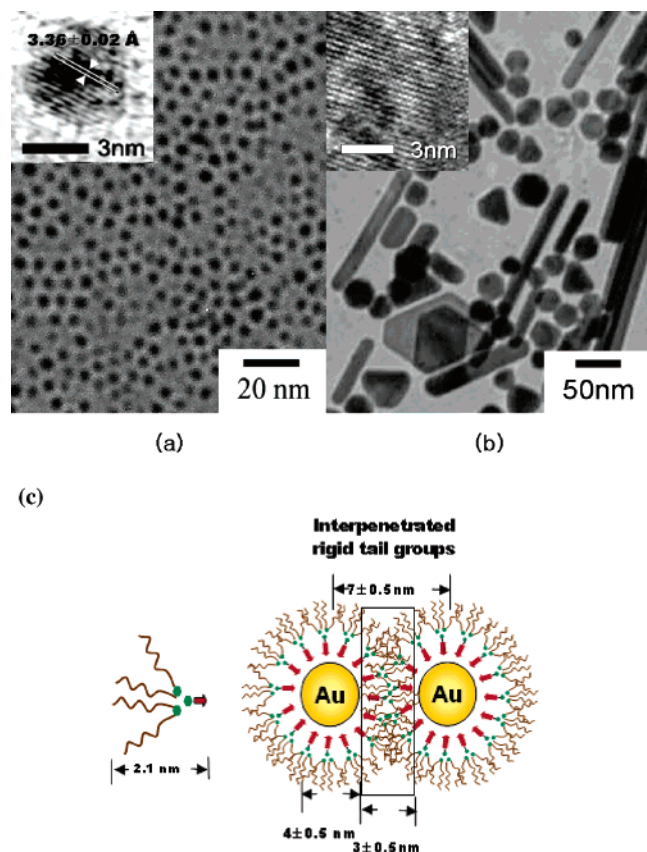


Figure 4. HR-TEM photographs of the 1-COOH-stabilized gold nanoparticles with a molar ratio ($\text{Au}^{\text{III}}/[\text{1-COO}^- - \text{Na}^+]$) of 1:2 after UV irradiation for (a) 48 h and (b) 72 h. Insets represent a higher magnification image of the Au lattice (d spacing of Au lattice is 2.36 \AA). (c) Schematic representation of the self-assembled 1-COOH-stabilized gold nanoparticles: the interpenetrated rigid tail groups of the molecules protecting neighboring nanoparticles.

differently in the solution state for the formation of ordered assemblies of 1-COOH-stabilized Au nanoparticles. The process by which the perfluorinated supramolecules are dissolved in solution, bind gold ions, and then after UV irradiation, bind metallic gold, is shown schematically in Scheme 1. First, dissolution of 1-COOH in THF (Scheme 1a) followed by neutralization with NaOH, yields the sodium salt (Scheme 1b). Then, the Au^{III} salt of 1-COOH is prepared by ion exchange from Na^+ into Au^{III} . In aqueous solution, a Cl^- ion or two Cl^- ions of AuCl_4^- seem to interact with the Na^+ ions of the $[\text{1-COO}^- - \text{Na}^+]$ complex, causing the AuCl_3^- or AuCl_2^- ions to form a composite in the presence of 1-COO^- (Scheme 1c,d). The conversion of the $[\text{1-COO}^- - \text{Na}^+]$ complex into the $[\text{1-COO}^- - \text{Au}^{\text{III}}\text{Cl}_3]^-$ complex generates an aggregated face-centered cubic (fcc) structure in THF. The structure and spacing of this structure are preserved during photoreduction by UV light. As a result, self-organization of the material with an organometallic core and perfluorinated tails gives rise to 1-COOH-stabilized gold nanoparticles (Scheme 1e), whose surfaces are completely covered with perfluorinated tails. Because the 1-COOH supramolecules act as passivation groups protecting against nanosize particle aggregation, the size of the final gold nanoparticles can be controlled during the reduction process (Scheme 1f).

Conclusion

In summary, ordered gold nanocrystals were prepared by an acid–base reaction and ion transfer reaction between a gold

salt and the core of a synthetic supramolecular template. By substituting the carboxylic core of the supramolecule with a Na^+ ion, followed by ion transfer of Au^{III} and subsequent reduction of Au^{III} with UV irradiation, an ordered supramolecule-based gold nanocomposite was generated. Well-ordered supramolecular self-assemblies of these types have many advantages: very small feature sizes (less than 10 nm) can be achieved, flexibility in regard to chemical functionality, easy control of orientation by surface anchoring, and fast response times to stabilize the molecular ordering and nanostructure due to the reversible and noncovalent interactions of the supramolecular molecules. The present approach using a self-assembled perfluorinated supramolecular template provides a new way to prepare metallic nanostructures. Furthermore, the nanoparticle spacing and shapes may be controllable, provided the supramolecular length can be controlled. Further studies of this strategy are in progress, aimed at controlling the particle spacing, shape, and preparing different types of metal and semiconductor nanoparticles.

Acknowledgment. This work was supported by MOCIE (RTI04-01-04), KOSEF (R01-2005-000-10456-0), and CUPSE-ERC. We also thank Prof. H. J. Song (KAIST, Chemistry) for helpful discussions. X-ray experiments performed at PLS (4C1 and 4C2 beam lines) were supported in part by MOST and POSCO.

Supporting Information Available: Detailed synthetic procedures, NMR spectra, and XRD profiles of (3,5-bis[p -(n -5,5,6,6,7,7,8,8,9,9,10,10,11,11,12,12-heptafluorododecan-1-yloxy)benzyloxy]benzoic acid) with structural analysis. This material is available free of charge via the Internet at <http://pubs.acs.org>.

References and Notes

- (1) Cao, G. *Nanostructures and Nanomaterials: Synthesis, Properties & Applications*; Imperial College Press: New York, 2004.
- (2) Yang, S. F.; Fan, L.; Yang, S. H. *J. Phys. Chem. B* **2004**, *108*, 4394.
- (3) Chiu, J. J.; Kim, B. J.; Kramer, E. J.; Pine, D. J. *J. Am. Chem. Soc.* **2005**, *127*, 5036.
- (4) Yoon, D. K.; Lee, S. R.; Kim, Y. H.; Choi, S.-M.; Jung, H.-T. *Adv. Mater.* **2006**, *18*, 509.
- (5) Yoon, D. K.; Jung, H.-T. *Langmuir* **2003**, *19*, 1154.
- (6) Xia, Y. N.; Yang, P. D.; Sun, Y. G.; Wu, Y. Y.; Mayers, B.; Gates, B.; Yin, Y. D.; Kim, F.; Yan, Y. Q. *Adv. Mater.* **2003**, *15*, 353.
- (7) Percec, V. *Chem. Rev.* **2001**, *101*, 3579.
- (8) Geissler, M.; Xia, Y. *Adv. Mater.* **2004**, *16*, 1249.
- (9) Choi, D.-G.; Jeong, J.-R.; Kwon, K.-Y.; Jung, H.-T.; Shin, S.-C.; Yang, S.-M. *Nanotechnology* **2004**, *15*, 970.
- (10) Kim, J.-U.; Cha, S.-H.; Shin, K.; Jho, J. Y.; Lee, J.-C. *Adv. Mater.* **2004**, *16*, 459.
- (11) Percec, V.; Glodde, M.; Bera, T. K.; Miura, Y.; Shiyanovskaya, I.; Singer, K. D.; Balagurusamy, V. S. K.; Heiney, P. A.; Schnell, I.; Rapp, A.; Spiess, H.-W.; Hudson, S. D.; Duank, H. *Nature* **2002**, *419*, 384.
- (12) Percec, V.; Glodde, M.; Johansson, G.; Balagurusamy, V. S. K.; Heiney, P. A. *Angew. Chem.* **2003**, *115*, 4474; *Angew. Chem., Int. Ed.* **2003**, *42*, 4338.
- (13) Kim, S. O.; Koo, J. M.; Chung, I. J.; Jung, H.-T. *Macromolecules* **2001**, *34*, 8961.
- (14) Daniel, M.-C.; Astruc, D. *Chem. Rev.* **2004**, *104*, 293.
- (15) Hudson, S. D.; Jung, H.-T.; Percec, V.; Cho, W.-D.; Johansson, G.; Ungar, G.; Balagurusamy, V. S. K. *Science* **1997**, *273*, 49.
- (16) Hudson, S. D.; Jung, H.-T.; Kewsuwan, P.; Percec, V.; Cho, W.-D. *Liq. Cryst.* **1999**, *26*, 1493.
- (17) Lee, S. R.; Yoon, D. K.; Park, S.-H.; Lee, E. H.; Kim, Y. H.; Stenger, P.; Zasadzinski, J. A.; Jung, H.-T. *Langmuir* **2005**, *21*, 4989.
- (18) Lee, E. H.; Yoon, D. K.; Jung, J.-M.; Lee, S. R.; Kim, Y. H.; Kim, Y. A.; Km, G.; Jung, H.-T. *Macromolecules* **2005**, *38*, 5152.
- (19) Tomalia, D. A. *Nat. Mater.* **2003**, *2*, 711.